Spacecraft Doppler Gravitational Wave Experiments

J. W. Armstrong

Jet Propulsion Laboratory,
California Institute of Technology, Pasadena CA 91109

Abstract. This paper discusses spacecraft Doppler tracking, the current-generation detection technique in the low-frequency gravitational wave band. Unlike other detectors, the ~1-10 AU earth-spacecraft separation makes the Doppler detector large compared with the gravitational wavelength; this has the consequence that the signal is time-resolved into three events in the Doppler time series. The principles of operation, including the transfer functions of the gravitational wave signal and the leading noise processes to the observed Doppler frequency time series, are outlined. Experiments-to-date, and the expected performance of the very-high-sensitivity Cassini experiment (to be done in 2001-2004) are discussed.

Doppler Tracking Technique in the Low-Frequency Band

Observations in the low-frequency (LF, ~0.00001-0.1 Hz) spectral band require space-based detectors. Currently the only broadband technique in the LF band is Doppler tracking of spacecraft. In this method, the earth and a distant spacecraft are free test masses in a "one-armed" interferometer, coherence being maintained through a high-precision frequency standard on the ground (1, 2, 3). The Doppler tracking system of the NASA Deep Space Network (DSN), referenced to an ultra-high-quality frequency standard, monitors a transponded microwave signal from a distant spacecraft. It thus continuously measures the relative dimensionless velocity ($2\,\Delta v/c = \Delta f/f_0$, where Δf is the Doppler shift and f_0 is the link center frequency) between the Earth and spacecraft. A gravitational wave of dimensionless strain amplitude h incident on the system causes small perturbations in the tracking record. These perturbations, of order h in $\Delta f/f_0$, are replicated three times in the Doppler data producing a geometry-dependent signature in the data (1), shown schematically in Figure 1. The sum of the Doppler perturbations of the three pulses is zero. Pulses with duration longer than about the one-way light time produce overlapping responses in the tracking record and the net response then cancels to first order. The tracking system thus has a passband to gravitational excitation: the low-frequency band edge depends on wave angle of arrival but is approximately set by pulse cancellation to be ~(1/two-way light time). Thermal (white phase noise in the receiver system) and frequency standard noise limit the high frequency band edge to about (1/10 seconds).

Response of Doppler System to Gravitational Wave Excitation

Unlike LISA, LIGO, or bar detectors, the ~1-10 AU earth-spacecraft separation makes the Doppler detector large compared with the GW wavelength for most candidate signals. In this regime, a GW incident on the Earth-spacecraft system resolves into three events in the Doppler time series: buffeting of the earth, buffeting of the spacecraft, and the initial buffeting of the Earth transponded back to the tracking station. Figure 1 shows this situation in cartoon form.

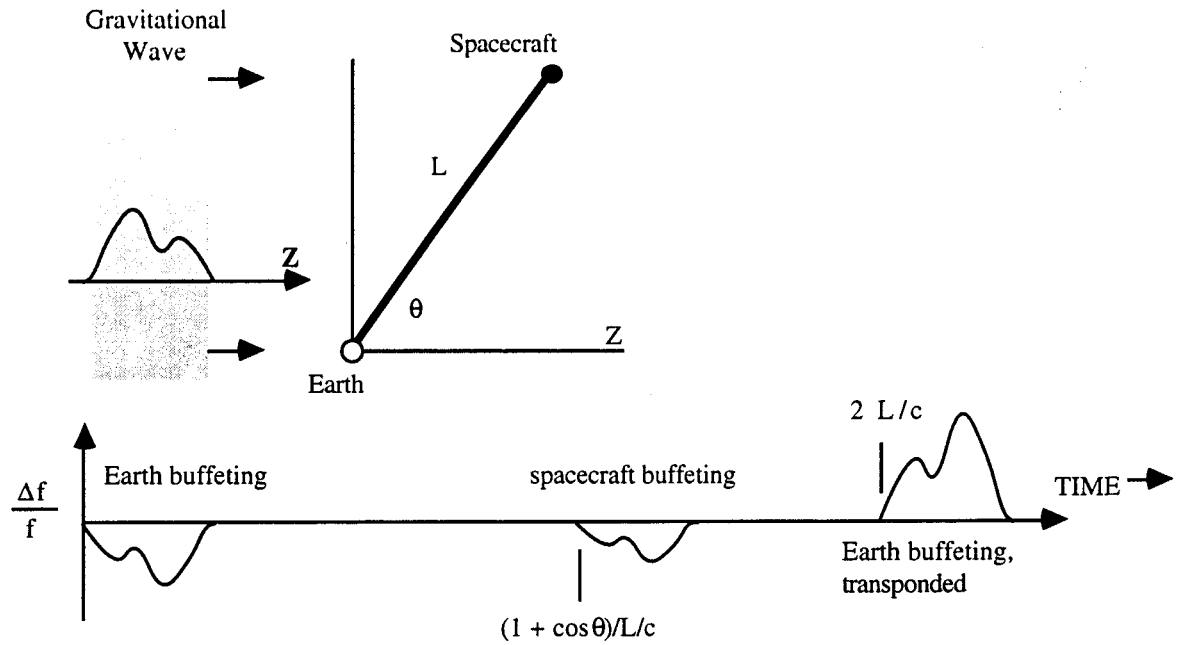

FIGURE 1. Schematic illustration of response of Earth-spacecraft tracking link to gravitational radiation having strain amplitude h. The Doppler perturbations are of order h in $\Delta f/f_0$ and, because the Earth-spacecraft separation is large compared with the GW wavelength, are resolved three times in the Doppler data: once when the wave "buffets" the earth, causing a small change in the difference between the transmitted and received Doppler frequencies, once when the spacecraft is buffeted by the wave, and finally when the initial earth perturbation is transponded back to the earth (1).

GWs compete with other perturbations of the Doppler time series. The noise level is quantified by the statistics of $y(t) = \Delta f/f_0$ for each noise process (4). Table 1 lists the principal noise processes in Doppler experiments and their transfer functions. These noise sources are: propagation noises (solar wind, ionosphere, troposphere--phase scintillation changes the apparent distance between the earth and spacecraft, hence $\Delta v/c$ hence $y(t) = \Delta f/f_0$), frequency standard noise (a fundamental noise, since interferometric techniques cannot be used to cancel it), antenna mechanical noise (unmodeled motion of the phase center as the ground antenna tracks the spacecraft), thermal noise (finite SNR often limits the high frequency sensitivity), and systematic errors. These noises enter the data through transfer functions connecting the noise process to the Doppler observable. Noise transfer functions are different from the transfer function for the GW signal--these differences can be exploited in signal processing for different gravitational signal waveforms. The way this is done depends on the dominant noise sources--their levels and spectral shapes--and on the signal characteristics. The dominant noise sources in turn depend on the technology used in the spacecraft and the ground stations. Previous generation experiments used an S-band (~2.3 GHz) tracking link. At this radio frequency plasma phase scintillation in the solar wind was the dominant noise source. Current generation experiments us X-band (~8.4 GHz) links, and are roughly equally affected by plasma scintillation noise and phase scintillation in the Earth's neutral atmosphere. Next generation experiments will use Ka-band (~32 GHz) and have independent tropospheric calibration and are expected to be limited by residual tropospheric calibration error and antenna mechanical noise. Analyses of the relevant noises have been published (5, 6, 7, 8, 9, 10).

In summary, a Doppler GW experiment residual time series (after removal of known effects) can be written as:

$$y(t) = \Delta f/f_0 = \text{gravity waves} + \text{propagation noise} + \text{clock noise} + \text{receiver thermal noise} + \text{systematic errors}$$

$$= \{[(\mu-1)/2]\,\delta(t) - \mu\,\delta[t-(1+\mu)L/c) + [(1+\mu)/2]\,\delta(t - 2L/c)\} * g(t)$$
$$+ \{\delta(t) + \delta[t-2L/c]\} * \text{troposphere}(t)$$
$$+ \{\delta(t) + \delta[t-2(L-x)/c]\} * \text{plasma}(t) + \{\delta(t) - \delta(t-2L/c)\} * \text{clock}(t)$$
$$+ \text{thermal}(t) + \text{systematic errors} \qquad (1)$$

where "$*$" indicates convolution, $g(t) = (1 - \mu^2)^{-1}\,\{\mathbf{n} \cdot [h_+(t)\,\mathbf{e}_+ + h_X(t)\,\mathbf{e}_X] \cdot \mathbf{n}\}$ is the scalar waveform produced by the polarized tensor wave's interaction with the earth-spacecraft system, **n** is a unit vector from Earth to the spacecraft, "troposphere", "plasma", "clock" and "thermal" are noise processes, L is the distance to the spacecraft, and x is the distance to the effective plasma "phase screen" ($x \approx 0.25$ AU for solar wind contribution in experiments done near solar opposition; $x \approx 0$ for the ionosphere).

TABLE 1. Principal Doppler perturbations in a GW experiment and their transfer functions. μ = cosine of the angle between the earth-spacecraft vector and the gravitational wave vector; L = earth-spacecraft distance, x = distance from the earth of equivalent plasma "screen" ($x = 0$ for the ionosphere; solar wind is an integral over x, but roughly $x \approx 0.25$ AU for observations at solar opposition).

Doppler perturbation	**time-domain transfer function**	**comment**
gravitational waves	$[(\mu-1)/2]\,\delta(t) - \mu\,\delta[t-(1+\mu)L/c) + [(1+\mu)/2]\,\delta(t - 2L/c)$	three pulse response--see Figure 1; see text following equation (1) for polarization coupling
plasma scintillation	$\delta(t) + \delta[t-2(L-x)/c]$	strongly dependent on link radio frequency; dominant noise process for S-band (~2.3 GHz) observations, comparable to raw troposphere for X-band (8.4 GHz), comparable to calibrated troposphere in Ka-band (32 GHz) experiments
tropospheric scintillation	$\delta(t) + \delta[t-2L/c]$	mostly due to water vapor (11); non-dispersive, thus does not improve as one goes to higher-radio frequency observations;
frequency standard ("clock noise")	$\delta(t) - \delta[t-2L/c]$	a fundamental limit; non-dispersive
antenna mechanical	$\delta(t) + \delta[t-2L/c]$	few observations (12); magnitude only approximately known
thermal	$\delta(t)$	level set by SNR on the up- and downlinks; along with frequency standard noise, sets high-frequency band edge
systematic errors and "other" effects	complicated (and in some cases transfer function concept is not applicable)	complicated

In situations where one of the noise processes is dominant, one can immediately see the correlation structure imposed on the Doppler data by its associated transfer function. X-band experiment sensitivity is set by a combination of soar wind plasma and tropospheric scintillation. Although the tropospheric noise is variable on time scales ~tracking pass length (or shorter) it can clearly show its transfer function (10). Figure 2 shows an example of Mars Global Surveyor data illustrating a strong tropospheric noise component. The two-way light time is 512 seconds, and the convolution of the time series with $\delta(t) + \delta[t-2L/c]$ produces an echo in the time series which shows up as positive correlation at the two-way light time. These transfer functions can be exploited in data analysis to improve sensitivity for some waveforms (1, 8, 22).

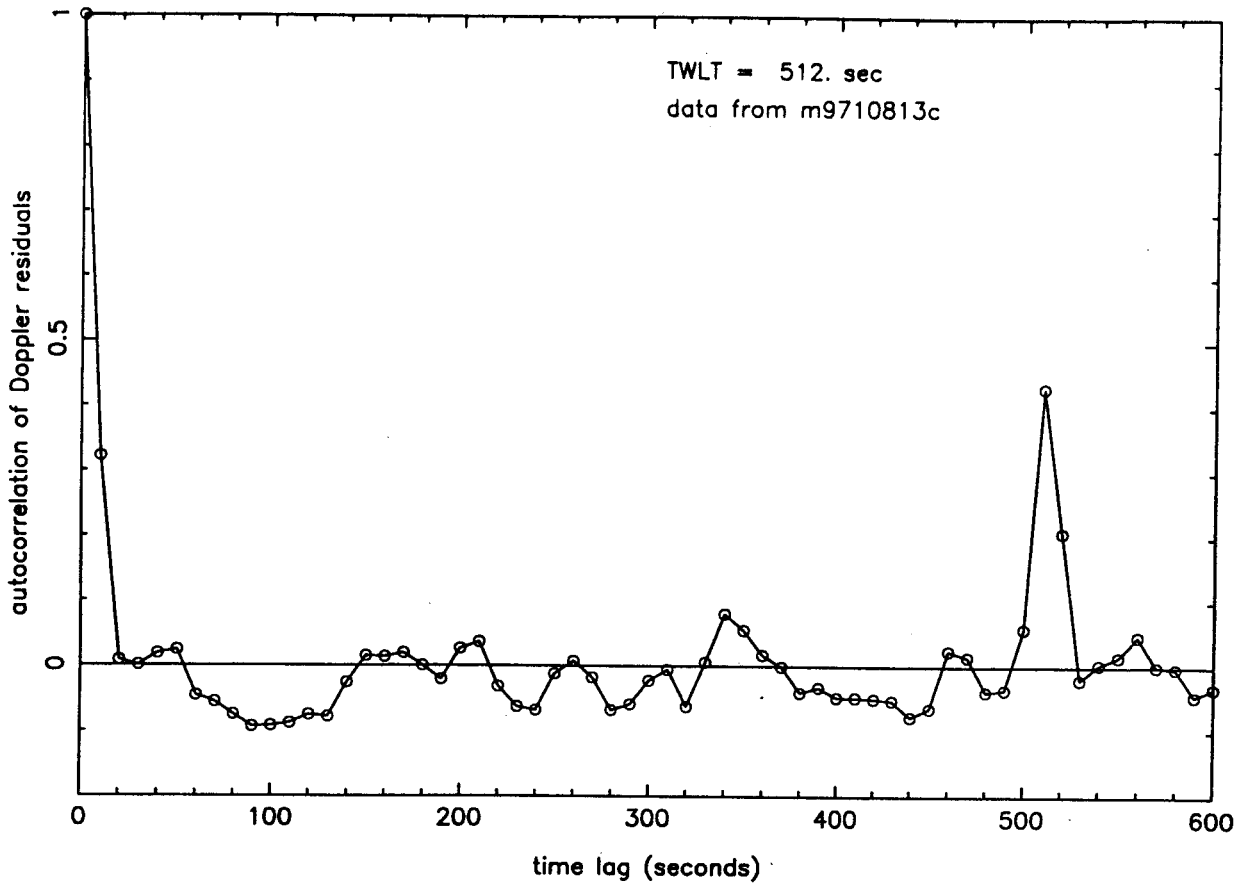

FIGURE 2. Autocorrelation function of X-band Doppler data from Mars Global Surveyor on 1997 DOY 108. The positive correlation at the two-way light time of 512 seconds is due to tropospheric scintillation and its transfer function (see text and Table 1). Differences in the transfer functions for the signal and the noises can be used to improve sensitivity (1, 8, 22)

Doppler Experiments

Spacecraft experiments require a distant spacecraft (low-frequency band edge is set by spacecraft range), a quiet cruising spacecraft (away from gravitational perturbations of a planet or nongravitational perturbations such as spacecraft thrusters), observations near the antisolar direction (to minimize plasma scintillation noise), and a high-stability ground system. Table 2 summarizes past and near-future Doppler observations. The sensitivity achieved depends the radio technology employed, the quality of the ground and spacecraft systems, the gravitational waveform, and the direction-of-arrival of the wave relative to the earth-spacecraft line. Current best sensitivity for, e.g., sinusoidal waveforms is slightly better than 10^{-15} over most of the low-frequency band for the Mars Observer (MO) data (17). The MO noise level is set by a combination of plasma scintillation noise and tropospheric scintillation. The Mars Global Surveyor (MGS) noise level should be somewhat lower than MO's (MGS was taken at larger sun-earth-spacecraft angle thus lower plasma noise) and MGS has better transfer function to, e.g., the galactic center direction.

The Cassini mission promises to improve significantly on X-band experiments. Cassini launched in October 1997 on a gravity assist (Venus-Venus-Earth-Jupiter) trajectory to Saturn. It has an elaborate radio system (20, 21), notably special hardware to allow Ka-band (~32 GHz) up- and down link capability. The NASA Deep Space Network is instrumenting one ground station (DSS 25, at Goldstone, CA) with a Ka-band uplink capability and an

advanced tropospheric calibration system to measure and calibrate most of the atmospheric scintillation. It is expected that these engineering improvements will give about an order of magnitude lowering of noise level relative to X-band experiments, with the level being set by residual uncertainty in the tropospheric calibration and antenna mechanical noise. Cassini's trajectory is such that it has three solar oppositions after the Jupiter gravity assist and before insertion into orbit around Saturn (December 16, 2001; December 27, 2002, and January 4, 2004). Cassini will be tracked for 40 days centered on each of these opposition opportunities. Cassini's right ascension at the oppositions will be 5h 34m, 6h 21m, and 6h 57m, while its declination will be $+22^{o}$ 39', $+21^{o}$ 51' and $+22^{o}$ 54'. The earth-spacecraft distance at these oppositions will be 5.7, 7.0, and 7.8 AU. The geometry is thus favorable for observations in the directions of most of the members of the Local Group (except, unfortunately, for the galactic center) and also for observations in the direction of Virgo. Additionally, the large two-way light time offers good transfer function to long period waves.

TABLE 2. Doppler GW experiments.

year of observation	spacecraft	comment
1980	Voyager	S-band uplink; a few tracking passes; burst search (13)
1981, 1988	Pioneer 10	S-band; 3 passes (1981); search for periodic waves at targeted frequency and direction; no GW from Geminga (14); 10 days of data (1988); search for chirp and coalescing binaries (15)
1983	Pioneer 11	S-band; 3 days of data; broadband search for periodic waves (16)
1992, 1993	Ulysses	S-band uplink, S/X band down link; 14 days in 1992, 19 days in 1993; part of 1993 coincidence experiment; search for all waveforms (2, 17)
1993, 1994, 1995	Galileo	S-band; 19 days in 1993, 40 days in 1994, 1995; part of 1993 coincidence experiment; search for all waveforms (18)
1993	Mars Observer	first X-band experiment; 19 days; part of 1993 coincidence experiment; search for all waveforms (19)
1997	Mars Global Surveyor	X-band; 21 days
2001, 2002, 2003	Cassini	first Ka-band experiment (advanced spacecraft radio system: X/Ka up and downlinks); 40 days per solar opposition; tropospheric calibration (20, 21)

Summary

Unlike other detectors, the Doppler GW antenna is large compared with the wavelength; thus there is a time-resolved three pulse response for the signal. The system is sensitive in the low frequency band, with geometry-dependent pulse cancellation setting the lowest frequency for full sensitivity to ~1/(two-way light time) (Figure 1) and link SNR (or the requirement to integrate long enough for good stability of the frequency standard) setting the high frequency limit to about 0.1 Hz.

The main noise sources are plasma scintillation noise, frequency standard noise, tropospheric scintillation noise, antenna mechanical noise; these enter the Doppler observations with transfer functions different than the GW (Table 1). The relative magnitude of these noise sources depends on the tracking technology employed. (For example, plasma phase scintillation in the solar wind dominate S-band (~2.3 GHz) observations.) The differences in the transfer function and in the noise levels can be used in signal processing design.

Current best sensitivity is achieved with X-band radio systems. X-band sensitivity is limited by a combination of tropospheric and plasma scintillation noises. The equivalent sinusoidal sensitivity for, e.g., Mars Observer, is slightly better than 10^{-15} over most of the LF band.

Cassini (Ka-band, 32 GHz radio link) will have strong suppression of plasma scintillation noise and a special tropospheric calibration system. Cassini is expected to be roughly 10 times more sensitive than X-band experiments and will probably be limited by residual ground antenna mechanical motion and residual uncalibrated troposphere.

To do significantly better than Cassini will require (a) moving all the test masses into space, (b) even higher-frequency links, and (c) an interferometric configuration to cancel the frequency standard noise. That is, Cassini is a very important improvement in the LF band but will probably be within a order of magnitude of the ultimate practical sensitivity of the Doppler GW technique. To improve on Cassini will require a LISA-like space-borne observatory.

Acknowledgments

The precision Doppler tracking capability is the result of work by many people. Crucial roles have been and are being played by individuals in the NASA Deep Space Network, the Flight Projects, and in the project radio science and radio science support teams. I thank in particular colleagues who were investigators on the Galileo/Mars Observer/Ulysses coincidence experiment: B. Bertotti, F. Estabrook, L. Iess, and H. Wahlquist. The research described here was carried out at the Jet Propulsion Laboratory, California Institute of Technology, under a contract with NASA.

References

1. Estabrook, F. B. and Wahlquist, H. D. *Gen. Rel. Grav.*, **6**, 439-447 (1975).
2. Bertotti, B., Ambrosini, R., Armstrong, J. W., Asmar, S. W., Comoretto, G., Giampieri, G., Iess, L. Koyama, Y., Messeri, A., Vecchio, A., and Wahlquist, H. D., *Astron. Astrophys.*, **296**, 13 (1995).
3. Iess, L. and Armstrong, J. W. "Spacecraft Doppler Experiments", in *Gravitational Waves: Sources and Detectors.*, I. Ciufolini and F. Fidecaro eds. (World Scientific, 1997), p. 323.
4. Barnes, J. A. *et al.*, Characterization of Frequency Stability, *National Bureau of Standards Technical Note 394*, Boulder CO, 1970.
5. Wahlquist, H. D., Anderson, J. D., Estabrook, F. B., Thorne, K. S., *Atti dei Covegni Lincei*, **34**, 335 (1977).
6. Estabrook, F. B. Gravitational Wave Detection with the Solar Probe. II. The Doppler Tracking Method, in *A Close-Up of the Sun*, edited by M. Neugebauer and R. W. Davies, pp. 441-449, JPL Publication 78-70 (1978).
7. Armstrong, J. W., Woo, R., and Estabrook, F. B., *Ap. J.*, **230**, 570 (1979) (erratum *Ap. J.* **240**, 719, 1980).
8. Armstrong, J. W. "Spacecraft Gravitational Wave Experiments" in *Gravitational Wave Data Analysis*, edited by B. Schutz, Dordrecht: Kluwer, 1989, pp. 153-172.
9. Riley, A. L. *et al.*, "Cassini Ka-Band Precision Doppler and Enhanced Telecommunications System Study", *Joint NASA/JPL/ASI Study on Ka-band*, Jet Propulsion Laboratory, Pasadena CA, 1990.
10. Armstrong, J. W. *Radio Science* (1998, in press).
11. Keihm, S. J., *TDA Progress Report*, **42-122**, 1-11 (1995).
12. Otoshi, T. Y., Franco, M. M., and Lutes, G. F., *Proc. IEEE*, **82**, 788 (1994).
13. Hellings, R. W., Callahan, P. S., and Anderson, J. D., *Phys Rev. D*, **23**, 844 (1981).

14. Anderson, J. D., Armstrong, J. W., Estabrook, F. B., Hellings, R. W., Lau, E. K., and Whalquist, H. D., *Nature*, **308**, 158 (1984).
15. Anderson, J. D., Armstrong, J. W., and Lau, E. K., *Ap. J.*, **408**, 287 (1993).
16. Armstrong, J. W., Estabrook, F. B., and Wahlquist, H. D., *Ap. J.*, **318**, 536 (1987).
17. Iess, L. and Armstrong, J. W. "Spacecraft Doppler Experiments", in *Gravitational Waves: Sources and Detectors.*, I. Ciufolini and F. Fidecaro eds. (World Scientific, 1997), p. 323.
18. Armstrong, J. W. "The Gallileo/Mars Observer/Ulysses Coincidence Experiment", to be published in *Second Amaldi Confernece on Graviational Waves*, E. Coccia *et al.* eds (World Scientific: Singapore), 1998.
19. Iess, L., Armstrong, J. W., Bertotti, B., Wahlquist, H. D., and Estabrook, F. B. "Search for Gravitational Wave Bursts by Simultaneous Doppler Tracking of Three Interplanetqary Spacecraft", talk presented at the *15th International Conference on General Relativity and Gravitation*, Pune, India December 16-21, 1997.
20. Comoretto, G., Bertotti, B., Iess, L., and Ambrosini, R., *Nuovo Cimento C*, **15**, 1193 (1992).
21. Bertotti, B., Comoretto, G., and Iess, L. Doppler Tracking of Spacecraft with Multifrequency Links, *Astron. Astrophys.*, **269**, 608 (1993).
22. Tinto, M. and Armstrong, J. W., *Phys. Rev. D*, (1998, in press).